Spectroscopic Exploration of Atomic Scale Superfluidity in Doped Helium Nanoclusters

A. R. W. McKellar,[1,*] Yunjie Xu,[2] and Wolfgang Jäger[2,†]

[1]*Steacie Institute for Molecular Sciences, National Research Council of Canada, Ottawa, Ontario K1A 0R6, Canada*
[2]*Department of Chemistry, University of Alberta, Edmonton, Alberta T6G 2G2, Canada*

(Received 11 September 2006; published 3 November 2006)

We present high resolution spectra of He_N-OCS clusters with N up to 39 in the microwave and 72 in the infrared regions, observed with apparatus-limited line widths of about 15 kHz and 0.001 cm^{-1}, respectively. The derived rotational constant, B (proportional to the inverse moment of inertia), passes through a minimum at $N = 9$, then rises due to onset of superfluid effects, and exhibits broad oscillations with maxima at $N = 24$, 47 and minima at 36, 62. We interpret these unexpected oscillations as a manifestation of the *aufbau* of a nonclassical helium solvation shell structure. These results bridge an important part of the gap between individual molecules and bulk matter with atom by atom resolution, providing new insight into microscopic superfluidity and a critical challenge for theory.

DOI: 10.1103/PhysRevLett.97.183401 PACS numbers: 36.40.Mr, 61.46.Bc, 67.90.+z

Unraveling how the property of superfluidity evolves from the atomic scale is a fundamental challenge and considerable progress has been made in recent years. The first attempt to determine the number of He atoms necessary for superfluidity to occur was the elegant "microscopic Andronikashvili experiment" [1], analogous to the pioneering measurements of bulk superfluid helium with a torsional oscillator disk [2]. Such helium nanodroplet experiments [3,4] carried out with mixed $H^4e/^3He$ droplets containing an embedded carbonyl sulfide (OCS) molecule were originally interpreted to indicate that a minimum of about 60 ^{4}He atoms were required for the onset of superfluidity [1]. The question of how many helium atoms are needed to induce superfluidity has begun to be answered in greater detail by high resolution microwave and infrared spectroscopy of $(helium)_N$-molecule clusters [5–8]. This work has also provided impetus (and experimental data) for theoretical studies [7–13] that have given first insights into details of the observed nonclassical behavior, and it now appears that the superfluid onset may take place in clusters with as few as 6 to 10 helium atoms, depending strongly on the probe molecule. High resolution cluster spectroscopy has long promised to bridge the gap between microscopic and macroscopic worlds through the study of successively larger clusters, but has thus far failed to deliver. We have now achieved a major step towards this goal with the study of the evolution of the bulk property superfluidity into the mesoscopic size regime.

OCS remains a favorite probe molecule for experimental [1,5,14–17] and theoretical [12,13,18–21] helium cluster studies. It is a strong chromophore in both the microwave and infrared (C-O stretch, $\approx$2062 cm^{-1}) regions, its rotational constant B is neither too large nor small, and He-OCS intermolecular forces are extensively characterized [19,22–25]. Our clusters are generated in pulsed supersonic jet expansions of dilute mixtures of OCS (<0.01%) in helium, with cooled jet nozzles (as low as $-140\,^\circ$C) and high backing pressures (up to 120 atmospheres). The infrared apparatus uses a tunable diode laser in a rapid-scan signal averaging mode [16,26] and is now configured with two vacuum chambers to skim the jet and reduce Doppler line broadening. The microwave apparatus is a Fourier transform spectrometer [27] incorporating improved double resonance capabilities based on signal decoherence by resonant pump radiation. Neither apparatus is explicitly able to distinguish different size clusters, so cluster size assignments depend on the variation of signal with jet conditions (lower jet temperature and higher backing pressure give larger N), and on spectral patterns.

Technical advances enabled the measurement of high resolution spectra of He_N-OCS clusters with N from 9 all the way up to 72. Figure 1 shows an overview of infrared results for the transitions $R(0)$ ($J = 1 \leftarrow 0$), $P(1)$ ($0 \leftarrow 1$), and $R(1)$ ($2 \leftarrow 1$), where J is the rotational quantum number. Remarkably, *every* $R(0)$ line is resolved and assigned in a monotonic progression from $N = 12$ to 72. Around $N = 21$, the lines are closely spaced but still resolved thanks to the skimmed jet. Beyond 72 the series continues, but the line spacing becomes too close to resolve. With higher backing pressures (not shown here), an unresolved 'lump' of $R(0)$ lines shifts further to the red, approaching the nanodroplet value [14] of 2061.79 cm^{-1}. The $P(1)$ and $R(1)$ series can be easily followed in many regions, but there are pile-ups of unresolved lines ($N = 25$–30 for $P(1)$, and 19–25 for $R(1)$) as well as regions hidden by unrelated lines. The patterns of hidden lines were estimated by means of simulated spectra, and confirmed by microwave results (discussed below) for the most important gaps. Some weaker $P(2)$ and $R(2)$ infrared transitions were also detected in the range $N = 12$–36.

Prominent $R(0)$ microwave transitions for the clusters with $N = 12$–20 were observed in the frequency region 3850–4700 MHz. In this size range, the B-value and infrared band origin change rapidly, facilitating unambiguous correlation of microwave and infrared results. Moreover, we detected the corresponding microwave

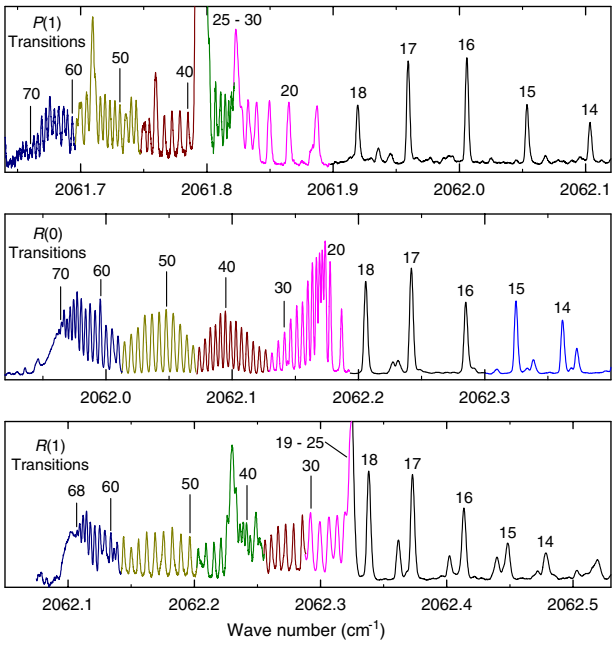

FIG. 1 (color online). Observed infrared spectra of He_N-OCS clusters, showing assigned cluster sizes, N. These spectra are montages where each color represents particular conditions (jet temperature and backing pressure) chosen to maximize the desired cluster sizes. For example, pink portions of each trace were taken with conditions favoring $N \approx 25$. Apparent variations in line strength are partly due to this montage. Effective rotational temperatures are ~0.2 K, even colder than the usual nanodroplet value of 0.37 K for ^{4}He. At these temperatures, the strongest features are the $R(0)$ transitions, shown in the central panel. The $P(1)$ and $R(1)$ series are shown in the upper and lower panels.

$R(1)$ transitions (7300 to 9000 MHz) and uniquely linked each $R(0)/R(1)$ pair by double resonance. Moving to larger clusters with appropriate experimental conditions, the microwave $R(0)$ series continued to higher frequencies, reaching He_{24}-OCS at 5048.567 MHz. The series then changed direction, moving to lower frequencies as N increased into the thirties. Microwave $R(0)$ transitions were detected up to $N = 39$, in excellent agreement with the infrared data but with much higher precision thanks to the narrow (≈15 kHz) microwave line width.

To summarize the experiments, there are earlier results [5,16,17] for $N = 1$–8, partial data for 9–11, and complete data for $N = 12$–72. The range 9–11 was difficult because signals are weak, the infrared spectrum is congested, and the microwave spectrometer is less sensitive in the required range (below 3 GHz). These difficulties introduce a slight uncertainty (± 1) in our absolute cluster size numbering above $N = 9$. However, for $N > 11$, the signals become strong again, and we can confidently assign each successive cluster size with excellent agreement between microwave and infrared data. For $N = 12$–20, each cluster has two linked microwave plus 4 or 5 infrared transitions, and for $N = 21$ to 39, a single microwave and 3 to 5 infrared transitions. For $N = 40$–70, there are 3 infrared transitions, which sometimes have to be interpolated through obscured regions. The observed transitions for $N > 11$ were adequately represented using a $K = 0$ symmetric top model with the following parameters: ν_0, the infrared band origin; B'' and B', the ground and excited C-O stretching state rotational constants; and $D = D'' = D'$ the centrifugal distortion parameter.

In Fig. 2, we plot the variation of B'' with number of helium atoms, N. Starting with $N = 0$–9, B'' drops (classically) as the cluster moments of inertia increase due to added He atoms. The turn-around at $N = 9$ signals the onset of superfluid effects, as helium density decouples from the overall rotational motion; this has also been observed in He_N-CO_2 and He_N-N_2O clusters [6–8]. The subsequent dramatic, nonclassical rise in B'' above the nanodroplet value is a clear indicator of increasing superfluid effects. A slight kink at $N = 14$ may be evidence of a structural effect, and a slope change at $N = 18$ may mark completion of the first solvation shell. B'' then reaches a local maximum centered at $N = 24$. A remarkable result in

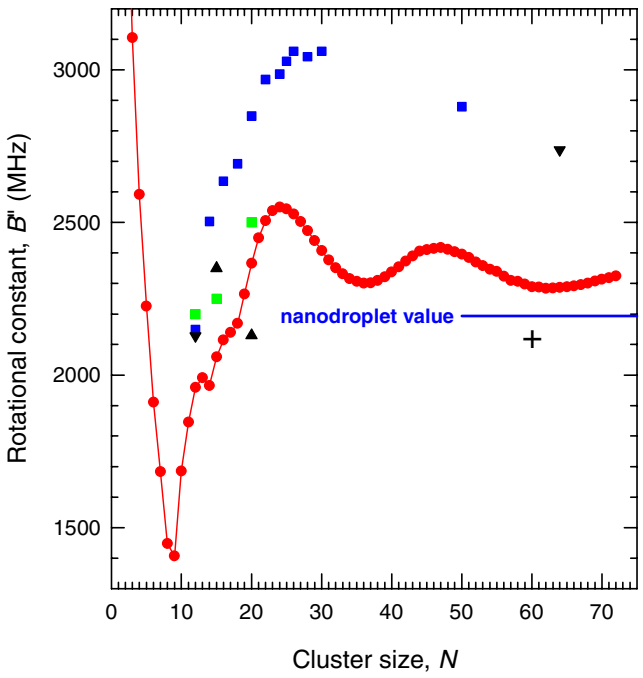

FIG. 2 (color online). Variation of the rotational constant B'' with cluster size. Experimental values (red circles) represent the present work, except for $N \leq 8$ [5]. The value observed [1] for $N \approx 60$ clusters within ^{3}He nanodroplets is shown as a black cross. It lies about 200 MHz below the free cluster value, and even below the usual nanodroplet value, perhaps due to added moment of inertia from "stray" ^{3}He atoms. Theoretical values for $N \geq 12$ are shown as black triangles [12,19], as inverted black triangles [20], as green squares [13], and as blue squares [21]. These fall in the right general region, but most are not particularly close to the observations.

Fig. 2 is the evidence of broad oscillations in B'' with maxima at $N = 24$, 47, and minima at 36, 62. There must be at least one further maximum (≈ 80) before B'' drops towards the nanodroplet value, and indeed there is evidence for further oscillations (not shown here) in the shape of the unresolved $R(0)$ "lump" mentioned above.

Theoretical results for B'' from state-of-the-art simulations by Paolini *et al.* [21] and others are shown in Fig. 2. While the first turn-around at $N \sim 9$ is captured, none of the simulations shows any indication of the oscillatory behavior observed here for $N > 20$. It is beyond the scope of this report to provide theoretical interpretations of these trends, which may indicate new physical phenomena in this size regime. Instead, we offer some qualitative observations. The oscillations are clear indication of the evolution of some sort of solvation shell structure. It is natural to associate a larger B-value (i.e., faster and less hindered rotation) with increased superfluid behavior (i.e., increased superfluid helium fraction, in a two-fluid model), and vice-versa. So it is tempting to link the minima in B with completed shells (relatively rigid and stable) and the maxima in B with half-filled shells (less rigidity, more fluidity). Inspection of the shell occupation numbers, however, indicates that these are not classical, i.e., purely structural, solvation shells, where one would expect a more drastic increase based on packing considerations. What is the nature of the solvation shell structure? Could addition of further helium atoms cause changes in helium densities (normal and superfluid) near the molecular impurity? In that case, the structure would strongly depend on the He-OCS interaction potential. Or is this structure a property of the emerging helium nanodroplet itself? In any case, it seems that the underlying physical mechanism is either lacking or not fully implemented in current simulations for this size regime. Theoretical predictions have in the past anticipated a rapid and smooth convergence of cluster properties to those of the nanodroplet [18,21], perhaps in part due to incorrect interpretation of results from the experiments on He_{60}-OCS clusters in ^{3}He nanodroplets [1], where B is already below the nanodroplet value (see below). We can now predict, from the observed trends and from the shape of unresolved line structure for $N > 72$, that there will be further structure in the evolution of spectroscopic observables (and cluster properties) towards the nanodroplet limit.

The *aufbau* of a helium solvation shell structure is further supported by the band origin results plotted in Fig. 3. For $N = 0$–5, the almost linear blue shift has been explained [5] as filling of a helium "donut ring" around the equator of the OCS molecule. This is followed by a turn-around to lower frequencies as He atoms occupy positions closer to the ends of the OCS. This red shift is roughly linear up to about $N = 19$, where there is a smooth but rapid change to a reduced slope, corresponding approximately to the filling of the first solvation shell. Close

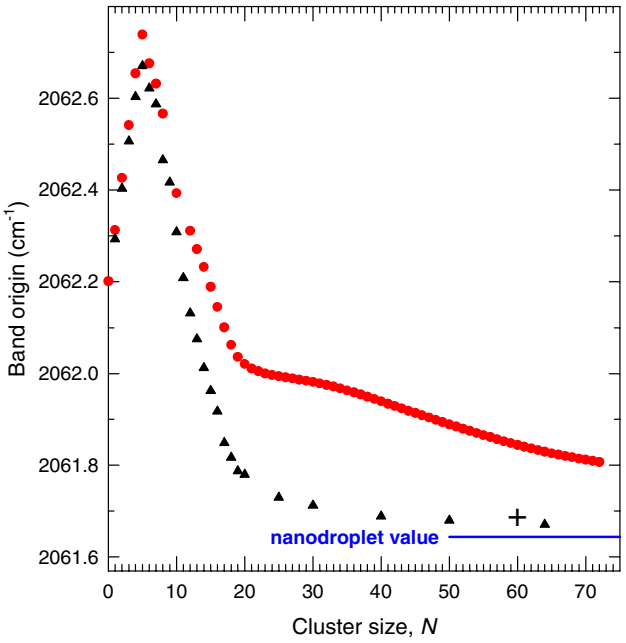

FIG. 3 (color online). Variation of the vibrational band origin with cluster size. Experimental values (circles) represent the present work, except for $N \leq 8$ [5]. Recent theoretical values [19] from diffusion Monte Carlo simulations (triangles) consistently overestimate the magnitude of red shift. The value observed [1] for $N \approx 60$ clusters within ^{3}He nanodroplets is shown as a black cross. This band origin is already close to the nanodroplet limit [14], not too surprising since it was obtained in a nanodroplet, albeit isotopically mixed.

inspection also reveals a slight slope change associated with the B'' minima ($N = 36$, 62). At $N = 70$, the vibrational origin is within 0.2 cm^{-1} of its observed [14] nanodroplet value.

Comparison of our cluster parameters with the results from the classic microscopic superfluidity experiment of Grebenev *et al.* [1] challenges some of the earlier conclusions. In that experiment [1], ^{3}He nanodroplets ($N \approx 10^4$) incorporating small numbers of ^{4}He atoms were probed by single OCS molecules. Because of zero point energy effects, the ^{4}He tended to coat the OCS, and when the estimated number of ^{4}He atoms reached about 60, the resolved free rotor infrared spectrum characteristic of ^{4}He (and of superfluidity) emerged from the featureless spectrum characteristic of ^{3}He. The band origin and rotational constant determined in Ref. [1] for $N \sim 60$ were about 2061.71 cm^{-1} and 2100 MHz, and these values are plotted as crosses in Figs. 2 and 3. Not surprisingly, this encapsulated band origin for $N \approx 60$ is close to the nanodroplet limit, since it was obtained in a nanodroplet (albeit isotopically mixed). The significance of the encapsulated B-value is less clear. It lies about 200 MHz below the free cluster value, and actually below the nanodroplet value, perhaps due to added moment of inertia from "stray" H^3e atoms. The biggest difference to the present results is that

our free clusters exhibit sharp structured rotational spectra for *all* values of $N < 72$. While it is evident that the sharp lines in the nanodroplet experiment indicate superfluid behavior, it is now clear that the earlier inference [1] that "the critical size of about 60 ^{4}He atoms [is] needed to permit molecular superfluidity" is incorrect. The present study shows that there is nothing special about cluster sizes around 60, in particular, in terms of line width, and that the observations that led to the earlier conclusion were a consequence of the ^{3}He matrix. The fact that the line widths in our cluster studies remain sharp up to $N = 72$, and probably higher, raises questions regarding the relationship between line width and superfluidity. The narrow line width also raises questions about nanodroplet line broadening. For OCS in ^{4}He nanodroplets, the $R(0)$ width is about 0.005 cm^{-1}, and while some of this may be due to droplet size distribution, there is good evidence [14] that this is not the major contributor. If transitions are sharp for $N = 72$ (and, we suspect, higher), but broadened for, e.g., $N = 6000$, and even more broadened for $N = 900$ (Ref. [14]), then what is the nature of this broadening, and at which cluster size does it become important? This question is of current interest [28] and our findings provide important experimental data for the debate.

The present results demonstrate that moderately large ($N \approx 100$) doped helium clusters can be produced in seeded supersonic jet expansions for direct microwave and infrared spectroscopic measurements, thus bridging a significant part of the gap between individual molecule and nanodroplet. This experimental breakthrough resulted in the striking observation of broad oscillations of the B-value in the range $N = 12$–72 (and probably higher). We interpret this unforeseen phenomenon in terms of the *aufbau* of a nonclassical superfluid helium solvation shell structure around the embedded OCS molecule. The experimental results provide an N by N sequence showing the complex evolution of superfluidity approaching the nanodroplet state.

We are grateful to N. Blinov, P.-N. Roy, J. K. G. Watson, and G. Scoles for stimulating discussions, and to H. Mäder for insights into the decoherence double resonance technique. This work was supported by the Natural Sciences and Engineering Research Council of Canada and the National Research Council of Canada.

*Electronic address: robert.mckellar@nrc-cnrc.gc.ca
†To whom correspondence should be addressed. Electronic address: wolfgang.jaeger@ualberta.ca

[1] S. Grebenev, J. P. Toennies, and A. F. Vilesov, Science **279**, 2083 (1998).
[2] E. L. Andronikashvili, J. Phys. USSR **10**, 201 (1946).
[3] J. P. Toennies and A. F. Vilesov, Angew. Chem. Int. Ed. Engl. **43**, 2622 (2004).
[4] C. Callegari, K. K. Lehmann, R. Schmied, and G. Scoles, J. Chem. Phys. **115**, 10 090 (2001).
[5] J. Tang, Y. Xu, A. R. W. McKellar, and W. Jäger, Science **297**, 2030 (2002).
[6] Y. Xu, W. Jäger, J. Tang, and A. R. W. McKellar, Phys. Rev. Lett. **91**, 163401 (2003).
[7] J. Tang, A. R. W. McKellar, F. Mezzacapo, and S. Moroni, Phys. Rev. Lett. **92**, 145503 (2004).
[8] Y. Xu, N. Blinov, P.-N. Roy, and W. Jäger, J. Chem. Phys. **124**, 081101 (2006).
[9] N. Blinov, X.-G. Song, and P.-N. Roy, J. Chem. Phys. **120**, 5916 (2004).
[10] S. Moroni, N. Blinov, and P.-N. Roy, J. Chem. Phys. **121**, 3577 (2004).
[11] E. W. Dreager and D. M. Ceperley, Phys. Rev. Lett. **90**, 065301 (2003).
[12] F. Paesani, A. Viel, F. A. Gianturco, and K. B. Whaley, Phys. Rev. Lett. **90**, 073401 (2003).
[13] S. Moroni, A. Sarsa, S. Fantoni, K. E. Schmidt, and S. Baroni, Phys. Rev. Lett. **90**, 143401 (2003).
[14] S. Grebenev, M. Hartmann, M. Havenith, B. Sartakov, J. P. Toennies, and A. F. Vilesov, J. Chem. Phys. **112**, 4485 (2000).
[15] S. Grebenev, M. Havenith, F. Madeja, J. P. Toennies, and A. F. Vilesov, J. Chem. Phys. **113**, 9060 (2000).
[16] Y. Xu and W. Jäger, J. Chem. Phys. **119**, 5457 (2003).
[17] J. Tang and A. R. W. McKellar, J. Chem. Phys. **119**, 5467 (2003).
[18] F. Paesani, F. A. Gianturco, and K. B. Whaley, J. Chem. Phys. **115**, 10 225 (2001).
[19] F. Paesani and K. B. Whaley, J. Chem. Phys. **121**, 4180 (2004).
[20] R. Zillich, F. Paesani, Y. Kwon, and K. B. Whaley, J. Chem. Phys. **123**, 114301 (2005).
[21] S. Paolini, S. Fantoni, S. Moroni, and S. Baroni, J. Chem. Phys. **123**, 114306 (2005).
[22] K. Higgins and W. Klemperer, J. Chem. Phys. **110**, 1383 (1999).
[23] J. Tang and A. R. W. McKellar, J. Chem. Phys. **115**, 3053 (2001).
[24] F. A. Gianturco and F. Paesani, J. Chem. Phys. **113**, 3011 (2000).
[25] J. M. M. Howson and J. M. Hutson, J. Chem. Phys. **115**, 5059 (2001).
[26] M. D. Brookes, C. Xia, J. Tang, J. A. Anstey, B. G. Fulsom, K.-X. A. Yong, J. M. King, and A. R. W. McKellar, Spectrochim. Acta, Part A **60**, 3235 (2004).
[27] Y. Xu and W. Jäger, J. Chem. Phys. **106**, 7968 (1997).
[28] K. K. Lehmann, Mol. Phys. **97**, 645 (1999).